Arch. Metall. Mater. **69** (2024), 3, 1261-1269

DOI: https://doi.org/10.24425/amm.2024.151761

B. KESKIN[1*], B. DERIN[2]

THERMODYNAMIC INVESTIGATION OF PROPAGATING BEHAVIOR IN SHS FOR EQUIATOMIC AND NON-EQUIATOMIC NiTi ALLOYS USING FACTSAGE SOFTWARE

In the current work, the thermodynamic properties of equiatomic and non-equiatomic Ni-Ti were estimated using Factsage Software for the "self-propagating high temperature synthesis (SHS) method. To calculate behind the pure substance model, the sublattice model was used. For the various ratios of the nickel in the B2 ordered phase and second intermetallics, the values of adiabatic temperature, Cp, Gibbs free energy, enthalpy of formation, products, and liquid-solid ratio were computed (Ni_3Ti, Ti_2Ni). These proporties play a crucial role in understanding the nature of propagating behavior since they affect the final product's micro/macrostructure, mechanical characteristics, and stable or metastable phases. The results were compared with the literature. It was also discussed why the existing studies could not reach the theoretical adiabatic temperature and the effect of the ignition W wire on the sample was investigated with the experimental study.

Keywords: NiTi; SHS; Thermodynamic; Combusting Synthesis

1. Introduction

NiTi is a very promising intermetallic material for the 21st century. It is well known for its shape memory effect. The transformation temperature for the alloy to regain its shape and amount of elongation can be controlled by various synthesis and post-treatment methods [1]. The mechanical properties depend on porosity, amount of deformation, and heat treatment. Additionally, it can alter the martensite/austenite start temperatures and transformation behavior [2,3]. The preheating is required for most of the intermetallics like NiTi before the ignition process because NiTi lacks the energy to be self-sustaining [4-7]. There are very limited studies have been carried out to predict the synthesis properties of NiTi by SHS. They mostly examined NiTi in pure substance form and calculated the enthalpy and adiabatic temperature values that can be achieved depending on the amount of pre-heating temperature [4,5,8,9]. These studies were limited to NiTi with an atomic ratio of Ni 50%- Ti 50%. However, Ni-Ti is an ordered crystal nucleated in the CsCl structure and has a wide solubility range above a certain temperature. As a result, increasing nickel in the Ni-Ti system changes the amount of liquid formed by the SHS method thus, it affects the macro/microstructure of the product. In this study, unlike the others, more precise calculations were made with help of the Factsage Thermodynamical Software program based on the idea that $Ni_xTi_{(1-x)}$ can dissolve in a wide range in the B2 phase structure. Thus, enthalpy, free energy, probability of reaction propagation, adiabatic temperatures, the products (NiTi, Ti_2Ni, Ni_3Ti) for equiatomic and non-equiatomic conditions were calculated and compared with existing experimental studies [10-16].

Studies conducted using SHS are not limited to pure powders. It is possible to obtain hard compounds (such as TiC, B4C, TaC) from low-value raw-materials [4,23]. Significant predictions can be made by utilizing software programs like Factsage, HSC, or Thermocalc to determine whether an adiabatic reaction will occur and to determine the final products [16-20].

There are numerous examples of such studies in the literature [23] Typically, starting from oxides, the reaction is expected to reach high temperatures through the assistance of an element that provides adiabatic energy, such as Al or Mg, and suitable products with appropriate affinity undergo the reaction [16]. Undesirable compounds are then drawn into the slag. It has been reported in the literature that the leaching process of undesired or slag-derived compounds is the major challenge in such studies [17].

[1] ISTANBUL MEDIPOL UNIVERSITY, VOCATIONAL SCHOOL, CONSTRUCTION TECHNOLOGY DEPARTMENT, ISTANBUL, TURKEY
[2] ISTANBUL TECHNICAL UNIVERSITY, METALLURGICAL AND MATERIALS ENGINEERING DEPARTMENT, ISTANBUL, TURKEY
* Corresponding author: bkeskin@medipol.edu.tr

2. Theoretical method

SGTE 2014 (for solid solution) and FactPs (for mostly pure elements and compounds) databases were used in the simulation, and equilibrium mode was preferred in Factsage Software for the calculations utilizing the Gibbs Free Energy Minimization method [10]. The thermodynamic model in the software was optimized based on a study by Bellen et al. [10,11]. In summary, the random solution can be described as Eq. (1):

$$\sum_{i=\mathrm{Ni,Ti}} x_i^{\varnothing} G_i^{\varnothing} + RT \sum_{i=\mathrm{Ni,Ti}} x_i^{\varnothing} \ln x_i^{\varnothing} + x_{\mathrm{Ni}}^{\varnothing} x_{\mathrm{Ti}}^{\varnothing} L_{\mathrm{Ni,Ti}}^{\varnothing} \quad (1)$$

Where $G_i^{\varnothing}$ is molar Gibbs energy, x is mole fraction, i can be Ni or Ti and L is the excess Gibbs energy, and can be expanded as the Redlich-Kister polynomial [12]. In the thermodynamic model: NiTi can be assumed as a complex B2 (ordered) phase with sub-lattices and it should be separately expressed behind the terminal (disordered) A2 phase. The end members of the B2 phase can be described as $(\mathrm{Ni{:}Ti})_{0.5}(\mathrm{Ni{:}Ti})_{0.5}(\mathrm{Va})_3$ and can be written as follows: Ni:Ti:Va, Ti:Ni:Va, Ni:Ni:Va and Ti:Ti:Va where Va stands for substitutional defects [11]. The B2 phase can be represented as Eq. (2):

$$\begin{aligned} G_m^{total} &= x_{\mathrm{Ni}}^{(1)} x_{\mathrm{Ni}}^{(2)} G_{\mathrm{Ni:Ni}}^{0} + x_{\mathrm{Ti}}^{(1)} x_{\mathrm{Ti}}^{(2)} G_{\mathrm{Ti:Ti}}^{0} + \\ &+ x_{\mathrm{Ni}}^{(1)} x_{\mathrm{Ti}}^{(2)} G_{\mathrm{Ni:Ti}}^{0} + x_{\mathrm{Ti}}^{(1)} x_{\mathrm{Ni}}^{(2)} G_{\mathrm{Ti:Ni}}^{0} + \\ &+ 0.5RT \begin{pmatrix} x_{\mathrm{Ni}}^{(1)} \ln x_{\mathrm{Ni}}^{(1)} + x_{\mathrm{Ti}}^{(1)} \ln x_{\mathrm{Ti}}^{(1)} + \\ + x_{\mathrm{Ni}}^{(2)} \ln x_{\mathrm{Ni}}^{(2)} + x_{\mathrm{Ti}}^{(2)} \ln x_{\mathrm{Ti}}^{(2)} \end{pmatrix} + G_m^{xs} \\ G_m^{xs} &= x_{\mathrm{Ni}} x_{\mathrm{Ti}} \sum_{i}^{n} L_{(\mathrm{Ti,Ni})}^{i} (x_{\mathrm{Ni}} - x_{\mathrm{Ti}})^i \end{aligned} \quad (2)$$

There are 4 end members in the calculation, but only the Ni:Ti:Va is stable. The other parts have never existed, and they can only be calculated using the sub-lattice model to better understand the formation of B2 [12-14]. Refer to Reference 10 or the most recent studies in References 12-13 for more information on the model and optimized thermodynamic data.

3. Experimental setup

To validate some of the thermodynamic studies, fundamental experiments are performed. For the experimental studies, Ni (Alfa Aeser, >99.8%, 44 μm) and Ti (Alfa Aeser, >99.5%, 150-250 μm) powder were used in equal atomic ratio, powder mixture was mixed in a tubular mixer for different time (TABLE 1). The diameter of the pellet pressed under 65-70 MPa pressure is 11.75 mm and the heights are various for the samples. The mixed powders were synthesized in a specially designed reactor in a protective argon atmosphere. A K-type thermocouple was placed in the middle of the sample from the outside and the pre-heating, ignition temperature and maximum temperatures reached were measured. The properties and SEM figures of the powders are in TABLE 1 and Fig. 1. Hitachi SU70 was utilized for powder images. Bruker D8 Advance X-Ray Diffractometer

TABLE 1

Properties of the Synthesis Samples

Samples	Pre-HeatIng Temp. (°C)	Ignition Temp./Mixed Temp. (°C)	Mass (g)	Mixture Time (h)	Heating Time (min)
S190	190	Null	4.7	4	28
S260	260	430	6.5	4	8.6
S240	240	Null	3	4	13.8
S150	150	330	3	4	12
S230	230	330	9.8	17	25.8

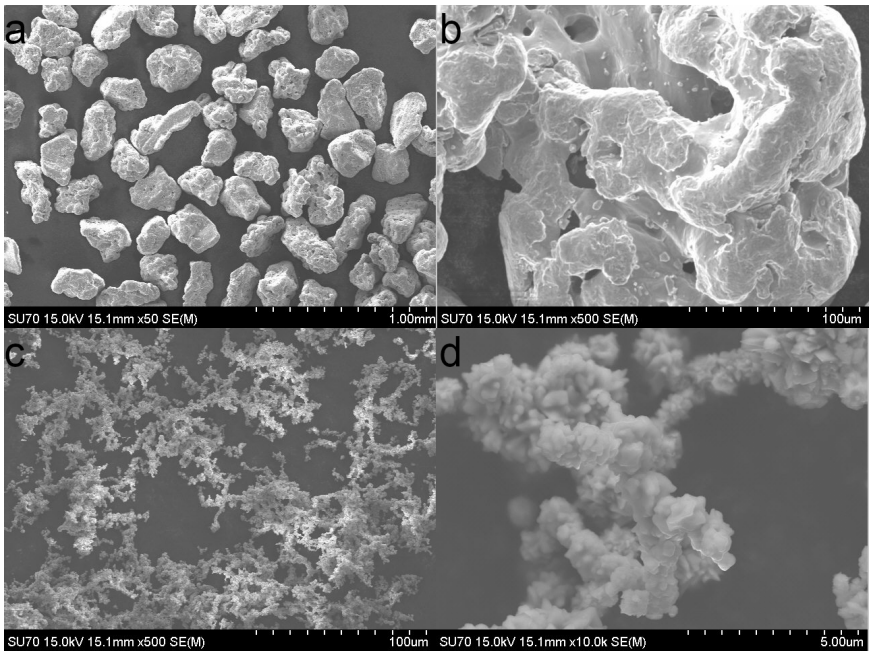

Fig. 1. SEM images of the powders, Ti (a, b); Ni (c, d)

was carried out to investigate structure at room temperature with Cu Kα radiation, and DSC Seiko 220C (heating rate of 10°/min, between –100°C and 150°C) was used to analysis phase transformation of the samples.

In the experiments, different pre-heating temperatures, mixing times, and amounts were compared with each other to understand the differences between thermochemical calculations and experiments. Thus, their effects on the obtained phases and maximum temperature were investigated. For the narrator's simplicity, short names are given to the samples. S means "sample" when the given number is the "preheating temperature".

4. Results

Fig. 2 shows the pre-heating temperature and time relationship of the 5 samples produced. The expression of data in smaller figures was prioritized by considering the time elapsed after ignition of the W wire in the samples, rather than focusing solely on the preheating temperature. As observed, the heating of the sample is influenced not only by the preheating temperature but also by the heating from the W wire. Consequently, the maximum temperature values attained are influenced by both factors, deviating from the values reported in the literature. It should be noted that the heating provided by the W wire is brief and may not result in homogeneous heating. Furthermore, the impact of the W ignition wire is more pronounced in smaller specimens. S150 proved it because S150 reached 330°C due to the W-wire and affected the whole specimen. As a result, it caused deformation with high liquid formation. Whereas in specimen S230, although it reached 330°C again, the specimen was less affected by this temperature and formed parallel slit lines due to the low pre-heating temperature and stopped halfway. In summary, although the results in the figure are written according to the pre-heating temperature, it should be thought that these values are a "mixed-heated" temperature and the smaller the sample, the more the W wire is under the heating effect. The samples can be seen in Fig. 3.

Samples (S150 and S240) made in 3 g and mixed for 4 hours in a tubular mixer were compared with each other. Although the W wire instantly became superheated, propagation of S240 was slower than the others. It has been noted that 150°C propagation is challenging in previous studies [5,6]. The reaction did not propagate spontaneously in the sample until it reached 330°C because the W ignition wire was not hot enough. In these samples, the propagation was smooth, and collapse was observed with partial melting because the mass of the samples was also low. Parallel slit was not observed in the specimen. Deformation was observed due to the high transition liquid in the shapes.

For comparison, the mass amount was increased by ~50% and S190 sample was synthesized at lower pre-heating temperatures. The propagation was achieved smoothly. The maximum temperature could not be recorded, it was observed that the W wire heated the sample, and the combustion synthesis was slow. Therefore, anisotropic parallel lines were observed. In other words, the formation of transition liquid in the reaction is low.

To better understand the heating effect of the W wire on the sample from the first studies produced, sample S260 was produced by increasing its mass to 6.5 gr. In this sample, the propagation occurred successfully when the W wire heated the sample to 430°C and the propagation stopped the near bottom. When Fig. 3 is examined, since the upper part was affected by 430°C, collapse and high melting occurred with high liquid formation, and circular regions were formed towards the lower parts. The structure is not anisotropic, probably due to high

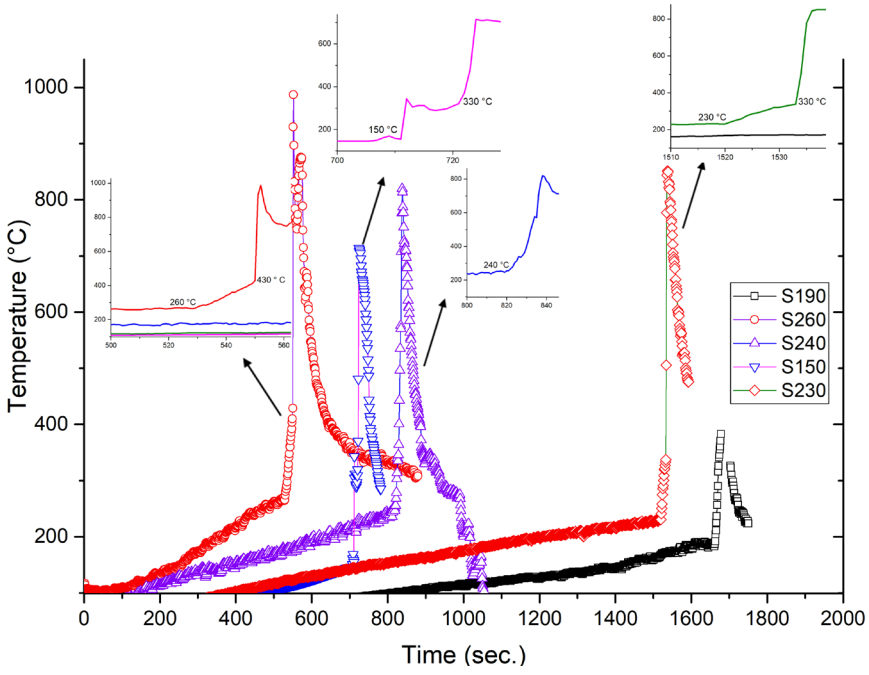

Fig. 2. Time-Temperature Profile of the samples

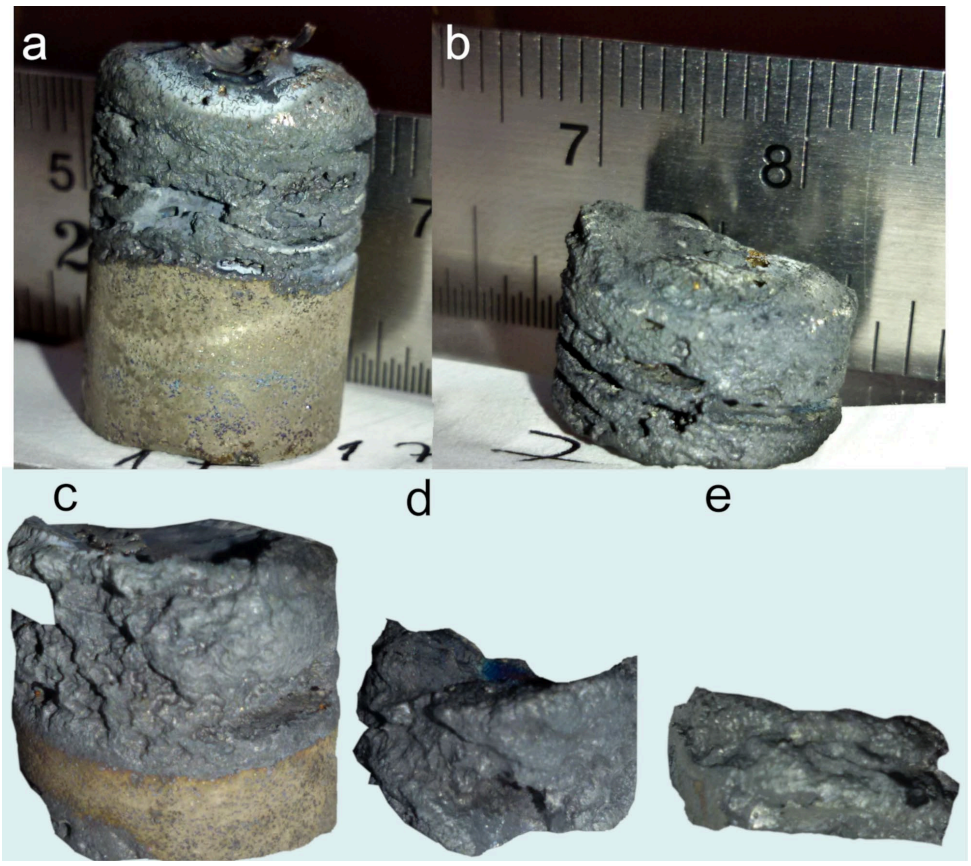

Fig. 3. Macrostructure of the outer surface of the sample; a – S230, b – S190, c – S260, d – S240, e – S150

transition liquid formation. Finally, the mass was increased by 50% to 9.8 g and the mixing time was increased ~4 times to 17 h. The sample was initially preheated to a temperature of 230°C (S230), and during the heating process facilitated by the W wire, a sudden propagation of the reaction was observed at 330°C. However, the propagation ceased prematurely, not reaching its complete extent.

S260 and S230 exhibited different results. A more anisotropic structure was obtained in S230 since the propagation started at 330°C, and the sample was longer. The reaction is influenced by the pre-heating temperature rather than the rapid heating temperature of the W wire. In general, the effect of the liquid/solid ratio and the shape and size of the parallel slit lines are more easily distinguished as the samples get longer.

The reason for the reaction to propagate halfway can be interpreted as the W wire only heats the sample halfway around 330°C. In other words, the unreacted part of the sample that could not be heated homogeneously by the W wire did not propagate. Also, oxidation of the interfaces in longer samples, resulting from the mixing of powders in an open atmosphere, may have hindered the reaction.

While the reaction is taking place, the slits parallel to each other parallel to the direction of heat propagation are noteworthy. The reason for this is shown in the literature to be the Kirkendall effect due to solid state diffusion and the vaporization of trapped gases [7,18,24]. In the case solid state diffusion, there is a little liquid formation in the reaction and the nickel diffuses faster than titanium, forming voids. The results are in line with previous studies [6,7,21,26].

The measured maximum temperatures were a little lower than expected. It possibly results from low pressing pressure (65-70 MPa), slow heating time (~25 min.) and the installation of the thermocouple. It was thought that the thermocouple touching from the outside could not measure the temperature sharply due to heat losses. Therefore, lower than expected values may have been obtained.

Fig. 4 shows the XRD analysis of the samples (mixed for 4 h, S190 and 17 h, S230) obtained after vertical cutting and polishing. While the main peak is B2, phases such as $T_{i2}Ni$ ($Ti_4Ni_2O_1$), and B19' phases are observed in the structure. Unreacted-free Ni and Ti powders are also obtained. A possible reason for this may be the large titanium powder size as reported in previous studies [5,6,26]. In addition, the dendritic structure of the nickel powders made it difficult to mix the powders and caused agglomeration. The reason for the $Ti_4Ni_2O_1$ phase may be the long heating time. Indeed, partial oxidation during the mixing process is also a possibility. Similar phases were also observed in sample S230. In the figure, although sample S190 was mixed for 4 hours, the free nickel content is very low and B19' martensite phase was observed at room temperature. At 150°C, these phases disappear. According to DSC analysis, As 84.7°C, Af 108.4°C, Ms 68.7°C and Mf 47.2°C were found in the sample. The enthalpy of transformation was calculated as ~11.39 mJ/mg. The values are consistent with the literature.

The propagation of S230 stopped halfway. The reasons can be listed as follows: 1 oxidation due to $Ti_4Ni_20_1$ and resistance to progress, 2 long heating time of 25.8 minutes, 3 high mixed time, the powders may have separated according to their mass. It should be noted that the XRD analysis showed a higher percentage of free nickel phase in sample S230.

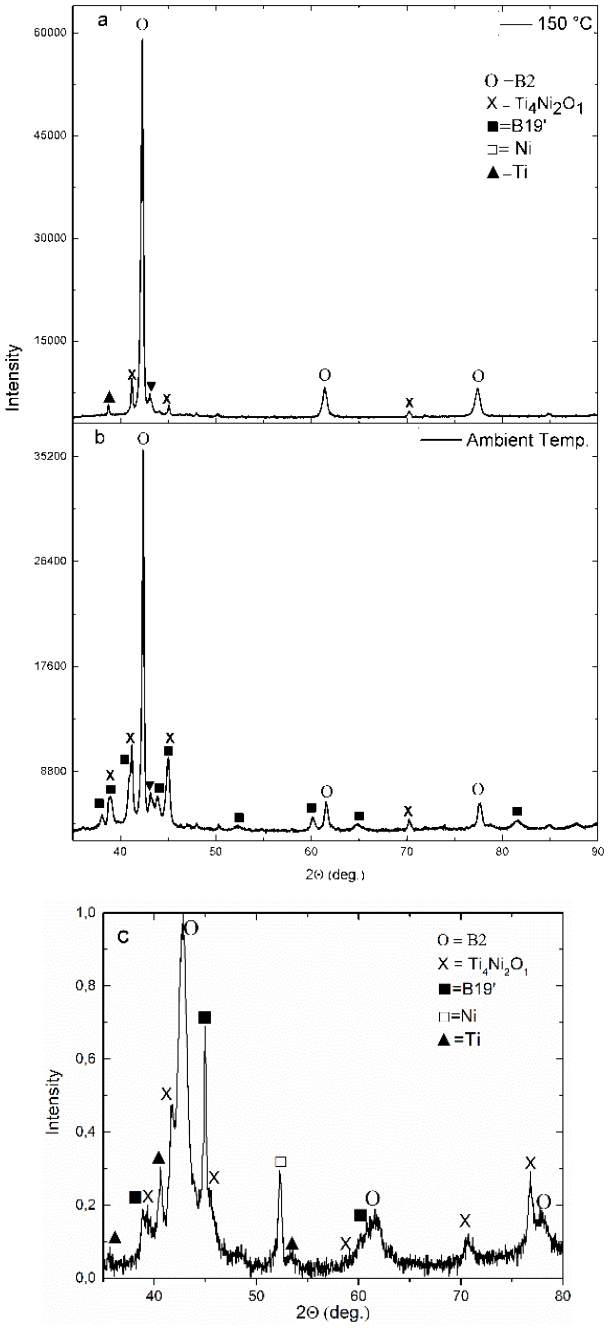

Fig. 4. XRD analysis of the sample. a-b – S190 at the ambient and 150°C temperature, S230 at ambient temperature

NiTi needs preheating for propagating before it is ignited because it does not have enough energy for self-sustaining. The condition of self-sustained is described as $\Delta H_{298}/Cp_{298} > 2000$ K or $T_{Ad} > 1800$ K (1523°C) where H is formation enthalpy (25°C) and Cp is the specific heat in constant pressure of the related phase [4]. Cp_{298} value is the key to the adiabatic temperature. The value of it calculated from the pure compound model was 46.7 kJ.(K.mol)$^{-1}$, while it was calculated as 50.01 kJ.(K.mol)$^{-1}$ by the sub-lattice model (in Factsage). The current studies on phase diagrams have been plotted utilizing the sub-lattice model [13,14]. Therefore, it should ensure more realistic results for the adiabatic temperature. The calculated thermodynamic properties are listed in TABLE 2.

TABLE 2

Comparison of previous studies with calculated thermodynamic properties of various $Ni_xTi_{(1-x)}$ phases

	$Ni_{0.5}Ti_{0.5}$	$Ti_{0.5}Ni_{0.25}$	$Ni_{0.75}Ti_{0.25}$
ΔG_f^0 (J/mol of atoms)	–34120.5[*] –32773[15]	–26546.7[*] –26010[15]	–36788[*] 33551[15]
Cp (J/(K.mol of atoms))	25.50[*] 25.52[11, 13] 23.37[15]	25.42[*] 24.71[13] 24.99[15]	25.62[*] 21.42[13] 23.37[15]
ΔH_f^0 (J/mol of atoms)	–34051.6[*] –34721[13] –34052[11] –33890[15]	–27222.4[*] –26977[13] –26901[11] –26777[15]	–37876.2[*] –42130[13] –36870[11] –34720[15]

[*] This work

In the Fig. 5, $\Delta H_{298}/Cp_{298}$ is calculated against the increase of nickel molar ratio in the B2 phase. The value of H/Cp as the B2 ordered phase is 1335.05 < 2000 K, therefore the reaction needs preheating. According to the calculated ratios, the NiTi phase is formed more easily than the Ti_2Ni phase, unlike the Gibbs free energy formation. However, in case of high nickel addition, the Ni_3Ti phase will form instead of NiTi. In the calculations, H/Cp decreases up to 0.333 molar ratio of Ni, which may be a misleading result because titanium is in the free state and does not contribute to enthalpy, while it contributes to Cp_{298}. It can be accepted as 1070.67 K for 1 mole of atoms (blue line). After a nickel molar ratio of 0.5, both NiTi (B2) and Ni_3Ti contribute to the enthalpy and the total enthalpy value increases negatively.

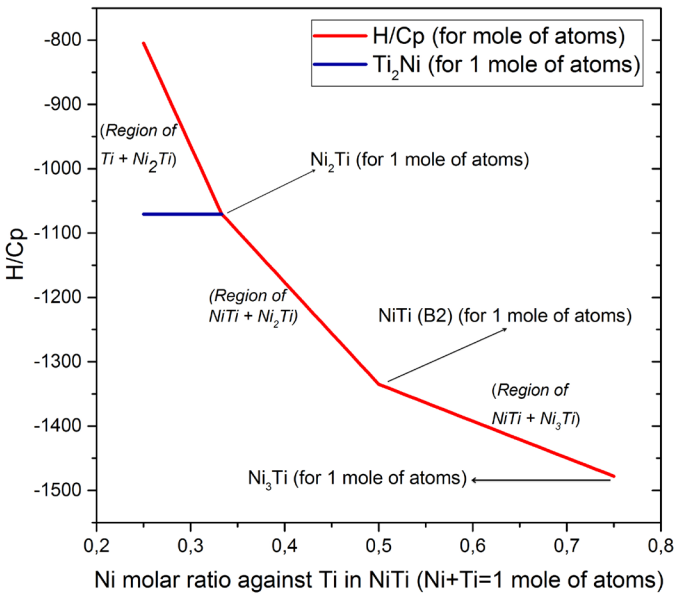

Fig. 5. H/Cp against molar ratio change of Ni in Ni-Ti mixture

In the first case, the powders are pure, and the mixture is homogeneous. The system works under 1 atm. without oxygen gases. The reaction takes place under adiabatic condition. The mass ratio of solid/liquid and adiabatic temperature against Ni molar ratio (in NiTi) is presented in Fig. 6.

Normalized mass ratios of solid and liquid are placed on the right y-axis and the adiabatic temperature is on the left y-axis. In Fig. 6, up until a point where the temperature is roughly 203°C, everything is completely solid. Since there were no transient liquids to form the dense product, the reaction is therefore driven by solid-state diffusion. It explains why the reaction was not propagated in the real experiment by Li et al. [5]. When the preheating temperature reaches 250°C and the adiabatic temperature reaches ~1308°C, a very small amount of liquid (L/S(mass) = 0.14) is formed. It was almost constant up until it reached 625°C, but the liquid-to-solid ratio kept increasing. There is no solid skeleton left after the formation of 100% liquid. The sample shows evidence of melting and losing its original shape. Temperatures between 203 and <625°C should be used to control porosity. In previous studies, Wisutmethangoon et al. reached a porosity of 37 and 31 vol.% in an experiment at under 200 and 300°C preheating temperatures (pressed 64 MPa) respectively [21]. Yeh et al. found the value of relative density value to be ~45% and ~83% for 100 and 300°C (for sample density 45%) preheating temperatures [6]. By the mean, if the preheating temperature is increasing, transient liquid way to control the density and porosities of the sample. In the present study, the liquid/solid ratio is about 22% for the sample that heated to 335°C, thus it is not enough to prevent the formation of the parallel slits in the real experiments. The main propagation mechanism is the solid-state diffusion. There are some controversial situations on it, which are argued in the next section.

In the second case, Fig. 7 illustrates the predicted changes in free energy for a mole of product at 25°C in both a and b. They are plotted for 0.25-0.75 moles of nickel, the Ni-Ti products bring the residual nickel up to 1 mole using titanium. The

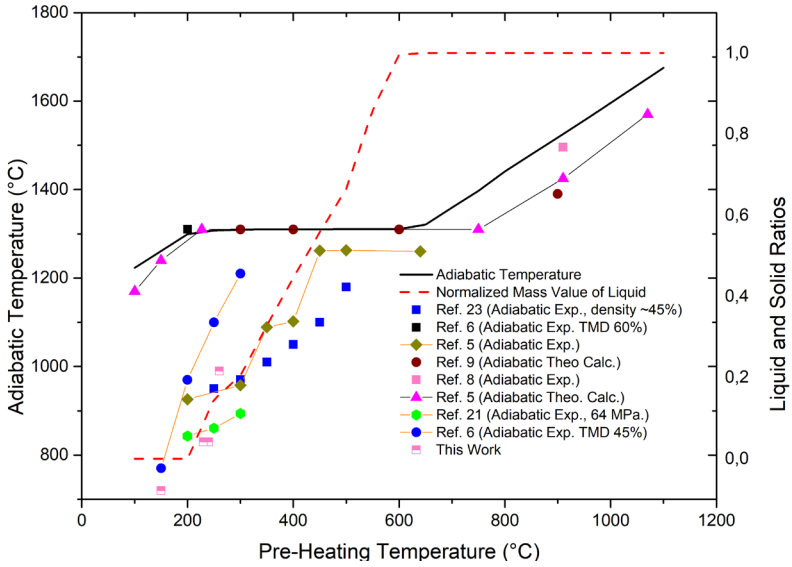

Fig. 6. Preheating temperature versus adiabatic temperatures related with change in amount of solid and transient liquid in NiTi

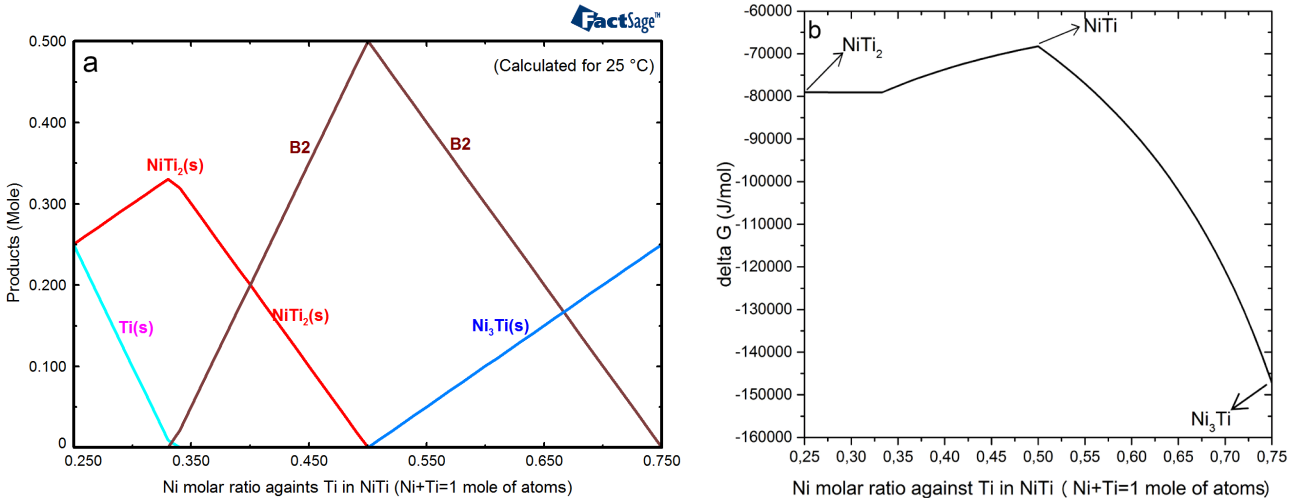

Fig. 7. (a) Products formed against molar ratio change of Ni in Ni-Ti mixture, (b) Gibbs free energy of a mixture of Ni (molar ratio) with Ti in NiTi system for 25°C

stable phases, as determined by the Gibbs free energy value, are $Ni_3Ti > Ti_2Ni > NiTi$. There is no Gibbs free energy change for per mole in the graph up to 0.333 because each nickel atom bonds 2 times as much titanium to form Ti_2Ni, and the remaining titanium precipitates without reacting. The creation of the Ni_3Ti phase next to NiTi causes the free energy to rapidly decline after a stoichiometric value of 0.5 mole of nickel. Only Ni_3Ti is produced when the nickel molar ratio is 0.75.

The formation of Ni_3Ti and Ti_2Ni is therefore inevitable in the SHS. Secondary phases appear where there are local deviations. When the end-member of the B2 lattice is observed during modeling, there is an increase in titanium-rich Ti:Ti:Va regions before 0.5 molar ratio and Ni:Ni:Va regions afterward. Upon reaching sufficient free energy, the Ni_3Ti phase becomes stable and appears alongside the B2 product.

The adiabatic temperature and the liquid-solid ratio calculations of non-equiatomic conditions are performed for the first time in this study. The adiabatic temperatures versus titanium versus nickel molar ratios are plotted (for Ni + Ti = 1 mole) in Fig. 8a, and liquid/solid (g/g) ratios are plotted in b. In the calculations, all nickel entered the B2 lattice and no by-products were formed. Up to 0.5 Ni, adiabatic temperatures increased and then decreased. With increasing nickel molar ratio, the liquid ratio decreased for each pre-heating temperature up to 0.5 molar ratios and then increased. The reason for this is that the adiabatic temperature enters the liquid+solid region. However, there is a transition from solid to liquid region at 0.5 molar ratios. From this modeling it can be concluded that the nickel-rich powder mixture will reach higher adiabatic temperatures than the titanium-rich mixture. No solid phase was observed after 0.5 Ni molar ratios at preliminary temperatures as high as 600°C.

5. Discussion

In Fig. 6, the adiabatic temperatures are different above 625°C when NiTi is considered as a stoichiometric compound instead of a solid solution. Especially in the experiments carried out by Yi and Moore at different powder sizes at the ignition temperature of 900°C, the adiabatic temperatures were found to be close to and just below the adiabatic temperatures calculated with the sub-lattice model. Therefore, the solution model is more realistic. Theoretically, in an adiabatic process, there is no energy or heat transfer to the surroundings, thus the amount of energy within the system remains constant. In real experiments, the heat is rapidly lost due to the conduction and radiation and is unable to exceed the calculated adiabatic temperature. Additionally, the particle size and compression amount affect the amount of heat within the structure.

In Fig. 6, the experimental maximum temperature is closer to the adiabatic temperatures with increasing initial temperature. As a hypothesis, when transient-liquid volume grows, voids close and heat conduction enhances. In samples with high initial density, a similar situation can be observed. Li et al. did not reach the melting point of NiTi between 200-650°C preheating temperature [5], whereas Yeh et al. (sample density 60%) and Chu et al. (with ignition reagent and 51 at.% Ni) reached the melting point at 200 and ~350°C respectively [6, 22]. They obtained a nearly dense product. It can also be supported with the present experimental study. In summary, when the preheating temperature is increased, it eliminates pores due to the occurrence of the more transient liquid, leading to more homogeneous heat transfer. Thus, the instantaneous maximum closes to the adiabatic temperature.

There are 2 conflicting results in NiTi synthesis. Some researchers argue that porosity increases with increasing preheating temperature [5,23-25], while others argue that it decreases [6,7,21,26, this study]. The probable reason for this is the sample sizes and heating rate studied. As a hypothesis: 1) The studies that showed an increase in porosity worked with a diameter of 2< cm while those that showed a decrease worked with a diameter of 1.2> cm. As the size increases, the number of places in the sample where the liquid can pass through and settle increases and localized large open porosities may be encountered. (2) The preheating temperature rate is also important corresponding to previous studies [24,26]. Tosun et al. have found that there is a limiting

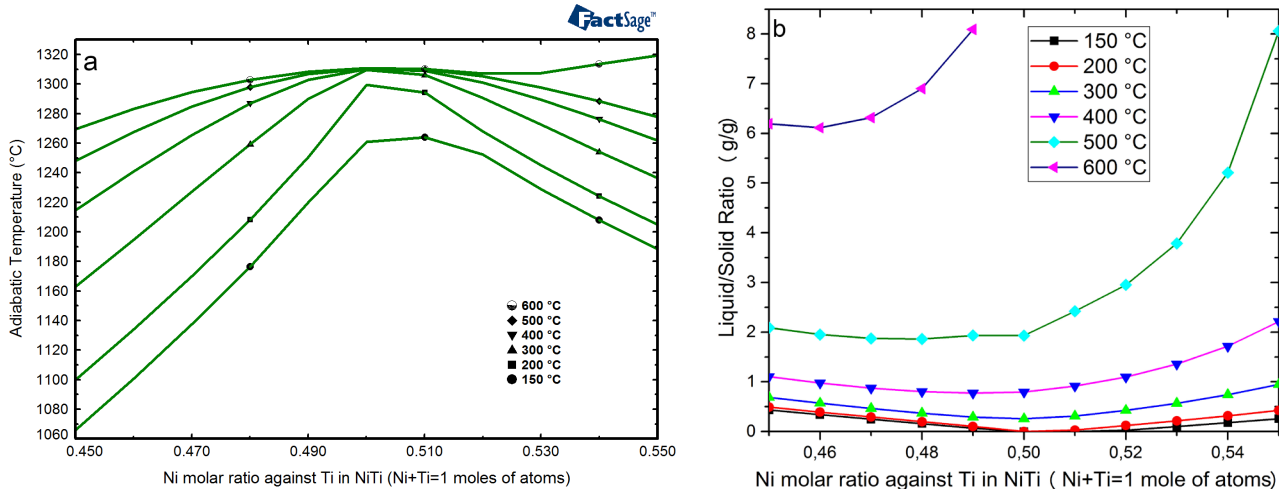

Fig. 8. (a) Adiabatic temperature, (b) liquid/solid mass ratio against molar ratio change of Ni in NiTi mixture

value for heating rate, beyond which there is an increase in porosity followed by a decrease for 10 mm green pellet. Especially with a decrease in pellet compression amount, this phenomenon becomes even more pronounced [27], a similar situation is also supported by Mossino et al. [18]. The reason for this may be the resistance created by powder compressed under low pressure, which hinders heat conduction. Munir et al. have reported that for several hard compounds (TaC, MoB, NiAl, MoS_2), the adiabatic temperature increases until a certain limit pellet diameter, after which it remains constant [4]. In the review article by Mossino et al., an increase in reaction rate was observed up to a critical thickness value for Ti-B mixture, followed by a decrease. The same article also observed a decrease in combustion rate and temperature, as well as sample swelling, with increasing pellet density in a the ($WO_3 + 3Zn \rightarrow 3ZnO + W$) reaction. It was noted that the swelling increased and the presence of parallel cracks became more pronounced as the diameter of the initial sample increased, which was attributed to the evaporation of Zn and the pressure of Argon gas. The observed anisotropy, which became more prominent with increasing preheating temperature [18], The reason for the increased presence of porosity in larger-sized NiTi samples may be attributed to this factor.

Novak et al. obtained 9% (±3) and 50% (±12) voids by volume in image analysis at heating rates of 300 and 20°C/min respectively at 1100°C by thermal explosion. In addition, the formation of by-products such as Ni_3Ti, Ti_2Ni increased in the case of slow heating regime [26,27]. This proves Fig. 7 because in the case of slow heating reaches lower combusting temperature, therefore the thermodynamic equilibrium approached. In the present study, the anisotropic slits are decreased when the preheating temperature is increased (see S230 vs S260) for the diameter of 11.75 mm.

Gibbs free energy and adiabatic temperature calculations alone do not provide sufficient insight into the propagation of the reaction. As can be seen in Fig. 5, H/Cp ratios were calculated against the molar ratio change of nickel. Under non-equiatomic circumstances, Ni_3Ti and Ti_2Ni might be more stable than NiTi, however the propagation of Ni_3Ti and NiTi in the SHS process is easier according to the Liquid/solid ratio shown in Fig. 7, but Ni_3Ti is formed at large stoichiometric deviations.

One of the important conclusions to be drawn is that Ni_3Ti can also be easily produced by SHS. The H/Cp ratio was found to be 1495 K. However, the porosity of the product is difficult to control because a high rate of liquid formation was calculated. The initial size of the sample is effective in forming a dense or hollow product, as previously explained. It can be said that if the B2 lattice is nickel-rich, porosity control will be difficult. It should be noted that porosity formation can also affect the Ms temperature [3].

6. Conclusions

In summary, using Factsage Software with the SGTE and FactPs databases, adiabatic temperatures, enthalpy, free energy, Cp values, liquid/solid ratios and the stable phases to be formed for equiatomic and non-equiatomic NiTi ratios with the sub-lattice model were calculated. For $Ni_{50}Ti_{50}$, it has been found that the liquid content increases with increasing preheating temperature, and previous and this experimental work has shown that this does not always lead to densification. The failure to reach the expected theoretical thermodynamic values in the past studies can be explained by the current studies and the experiment as follows:

1) The main reasons are dimensions of the green sample and pre-heating temperature. The higher pre-heating temperature leads to a higher instantaneous maximum temperature which is more convenient with the (theoretical) adiabatic temperature. The formation of the transient liquid eliminates losses due to the pores. In the present studies, the lower preheating temperature (as S190, S230 and S260) leads to the lower instantaneous maximum temperature.
2) The powder size and the dendritic nature of the powder made mixing difficult and as a result, free Ni and Ti phases beside Ti_2Ni were found in XRD analysis. Especially in the experiments with W, the sample is heated up because of the trigger wire not reaching the expected temperature immediately. The small specimens were more affected by the W wire and the pores were formed accordingly, while the large specimens were affected by the mixed temperature (Heat of pre-heating+W ignition wire).

The porosity of products with increasing nickel content is difficult to control with increasing liquid content because high liquid content is reached. H/Cp, Gibbs free energy, and products formed were calculated for room temperature with nickel molar ratio ranging from 0.25 to 0.75. It was found that $\Delta G_f^0(Ni_3Ti) > \Delta G_f^0(Ti_2Ni) > \Delta G_f^0(NiTi)$, but when the probability of the reaction propagating on its own (H/Cp) is investigated, the order Ni_3Ti>NiTi>Ti_2Ni was reached. These results explain why secondary intermetallics are formed in NiTi synthesis. It has been shown that Ni_3Ti is suitable for SHS fabrication with a high H/Cp ratio.

Acknowledgments

The authors are pleased to acknowledge the financial support from The Scientific and Technological Research of Turkey (TUBITAK, Project No: 213M556).

REFERENCES

[1] M.H. Elahinia, M. Hashemi, M. Tabesh, S.B. Bhaduri, Manufacturing and processing of NiTi implants: A review. Progress in Materials Science **57**, 911-946 (2012). DOI: https://doi.org/10.1016/j.pmatsci.2011.11.001

[2] H. Jiang, L. Rong, Ways to lower transformation temperatures of porous NiTi shape memory alloy fabricated by self-propagating

high-temperature synthesis. Materials Science Engineering **438**, 883-886 (2006).
DOI: https://doi.org/10.1016/j.msea.2006.01.103

[3] B. Yuan, X. Zhang, C.Y. Chung, M. Zhu, The effect of porosity on phase transformation behavior of porous Ti–50.8 at.% Ni shape memory alloys prepared by capsule-free hot isostatic pressing. Materials Science Engineering: A **438**, 585-588 (2006).
DOI: https://doi.org/10.1016/j.msea.2006.02.141

[4] Z.A. Munir, U. Anselmi-Tamburini, Self-propagating exothermic reactions: the synthesis of high-temperature materials by combustion. Materials Science Reports **3** (7-8), 277-365 (1989).
DOI: https://doi.org/10.1016/0920-2307(89)90001-7

[5] B. Li, Rong, L.J., Y.-Y. Li, V. Gjunter, Synthesis of porous Ni–Ti shape-memory alloys by self-propagating high-temperature synthesis: reaction mechanism and anisotropy in pore structure. Acta Materialia **48** (15), 3895-3904 (2000).
DOI: https://doi.org/10.1016/S1359-6454(00)00184-1

[6] C.L. Yeh, W.Y. Sung, Synthesis of NiTi intermetallics by self-propagating combustion. Journal of Alloys and Compounds **376** (1-2), 79-88 (2004).
DOI: https://doi.org/10.1016/j.jallcom.2003.12.016

[7] B.Y. Tay, C.W. Goh, Y.W. Gu, C.S. Lim, M.S. Yong, M.K. Ho, M.H. Myint, Porous NiTi fabricated by self-propagating high-temperature synthesis of elemental powders. Journal of Materials Processing Technology **202** (1-3), 359-364 (2008).
DOI: https://doi.org/10.1016/j.jmatprotec.2007.09.037

[8] J.J. Moore, H.C.Yi, Combustion Synthesis and Its Application in Producing Intermetallic Shape Memory Alloys. Materials Science Forum **56-58**, 637-642 (1990).
DOI: https://doi.org/10.4028/www.scientific.net/MSF.56-58.637

[9] L. Zhang, Z. Wang, Thermal investigation of fabricating porous NiTi SMA by SHS. Experimental Thermal and Fluid Science **32** (6), 1255-1263 (2008).
DOI: https://doi.org/10.1016/j.expthermflusci.2008.02.006

[10] C. . Bale, E. Bélisle, P. Chartrand, S.A. Decterov, G. Eriksson, A. Gheribi, K. Hack, I.-H. Jung, Y.-B. Kang, J.J.C. Melançon, Reprint of: FactSage thermochemical software and databases 2010-2016. **55**, 1-19 (2016).

[11] P. Bellen, K.H. Kumar, P. Wollants, Thermodynamic assessment of the Ni-Ti phase diagram. International Journal of Materials Research **87** (12), 972-978 (1996).
DOI: https://doi.org/10.1515/ijmr-1996-871207

[12] N. Saunders, A. P.Miodownik (Ed.), CALPHAD (calculation of phase diagrams): a comprehensive guide, 1998 Elsevier.

[13] E. Povoden-Karadeniz, D. Cirstea, P. Lang, T. Wojcik, E. Kozeschnik, Thermodynamics of Ti–Ni shape memory alloys. Calphad **41**, 128-139 (2013).
DOI: https://doi.org/10.1016/j.calphad.2013.02.004

[14] W. Tang, B. Sundman, R. Sandström, C. Qiu, New modelling of the B2 phase and its associated martensitic transformation in the Ti–Ni system. Acta Materialia **47** (12), 3457-3468 (1999).
DOI: https://doi.org/10.1016/S1359-6454(99)00193-7

[15] I. Barin, G. Platzki, Thermochemical data of pure substances, 1989 Wiley Online Library, Weinheim.

[16] O. Çoban, M. Buğdaycı, M.E. Açma, Production of B4C-TiB2 composite powder by self-propagating high-temperature synthesis. Journal of the Australian Ceramic Society **58**, 777-791 (2022).
DOI: https://doi.org/10.1007/s41779-022-00714-5

[17] O. Çoban, M. Buğdaycı, S. Başlayıcı, M.E. Açma, Combustion Synthesis of B4C TiB2 Nanocomposite Powder Effect of Mg Particle Size on SHS and Optimization of Acid Leaching Process. Journal of Superhard Materials **45**, 20-40 (2023).
DOI: https://doi.org/10.3103/S1063457623010033

[18] P. Mossino, Some aspects in self-propagating high-temperature synthesis. Ceramics International **30**, 311-332 (2004).
DOI: https://doi.org/10.1016/S0272-8842(03)00119-6

[19] Ö.C. Odabaş, M. Buğdaycı, S. Kan, A. Turan, O. Yücel, Effects of reductant type on the combustion synthesis of NiB. Solid State Sciences **111**, 1-8 (2021).
DOI: https://dx.doi.org/10.1016/j.solidstatesciences.2020.106447

[20] M. Buğdaycı, G. Deniz, C. Ziyreker, A. Turan, L. Öncel, Thermodynamic modeling and production of FeCo alloy from mill scale through metallothermic reduction. Engineering Science and Technology, an International Journal **23**, 1259-1265 (2020).
DOI: https://doi.org/10.1016/j.jestch.2020.03.003

[21] S. Wisutmethangoon, N. Denmud, L. Sikong, Characteristics and compressive properties of porous NiTi alloy synthesized by SHS technique. Materials Science and Engineering: A **515** (1-2), 93-97 (2009).
DOI: https://doi.org/10.1016/j.msea.2009.02.055

[22] C.L. Chu, C.Y. Chung, P.H. Lin, S.D. Wang, Fabrication of porous NiTi shape memory alloy for hard tissue implants by combustion synthesis. Materials Science and Engineering: A **366** (1), 114-119 (2004). DOI: https://doi.org/10.1016/j.msea.2003.08.118

[23] C.-L. Chu, B. Li, S.-D. Wang, S. Zhang, X. Yang, Z. Yin, Preparation of TiNi shape memory alloy porosint by SHS. Transactions of the Nonferrous Metals Society of China **7** (4), 84-87 (1997).

[24] A. Biswas, Porous NiTi by thermal explosion mode of SHS: processing, mechanism and generation of single phase microstructure. Acta Materialia **53** (5), 1415-1425 (2005).
DOI: https://doi.org/10.1016/j.actamat.2004. 11.036

[25] Y.-H. Li, L.-J. Rong, Y.-Y. Li, Pore characteristics of porous NiTi alloy fabricated by combustion synthesis. Journal of alloys and Compounds **25** (1), 259-262 (2001).
DOI: https://doi.org/10.1016/S0925-8388(01)01382-2

[26] P. Novák, L. Mejzlíková, A. Michalcová, J. Čapek, P. Beran, D. Vojtěch, Effect of SHS conditions on microstructure of NiTi shape memory alloy. Intermetallics **42**, 85-91 (2013).
DOI: https://doi.org/10.1016/j.intermet.2013.05.015

[27] G. Tosun, L. Ozler, M. Kaya, N. Orhan, A study on microstructure and porosity of NiTi alloy implants produced by SHS. Journal of Alloys and Compounds **487**, 605-611 (2009).
DOI: https://doi.org/10.1016/j.jallcom.2009.08.023